Struct Multidisc Optim (2018) 57:39–54
https://doi.org/10.1007/s00158-017-1849-3

RESEARCH PAPER

Multi-objective probabilistic optimum monitoring planning considering fatigue damage detection, maintenance, reliability, service life and cost

Sunyong Kim[1] **· Dan M. Frangopol**[2]

Received: 6 June 2017 / Revised: 17 October 2017 / Accepted: 24 October 2017 / Published online: 10 November 2017

Abstract Effective and efficient service life management is essential for a deteriorating structure to ensure its structural safety and extend its service life. The difficulties encountered in the service life management are due to the uncertainties associated with detecting and identifying structural damages, and assessing and predicting the structural performance. To reduce these uncertainties, continuous long-term structural health monitoring (SHM) can be employed. However, a rational and practical SHM planning is required to simultaneously maximize the accuracy, efficiency, and cost-effectiveness in service life management. This paper proposes a probabilistic optimum SHM planning based on five objectives to be simultaneously optimized: minimizing the expected damage detection delay, minimizing the expected maintenance delay, maximizing the damage detection time-based reliability index, maximizing the expected service life extension, and minimizing the expected life-cycle cost. The formulations of the five objectives are based on the probabilistic fatigue damage assessment. The monitoring plannings associated with both a single- and a multi-objective probabilistic optimization process (MOPOP) are investigated. For efficient decision making in identifying the essential objectives and selecting a well-balanced solution among the Pareto optimal solutions, the degree of conflict among objectives and objective weights are estimated. The novel approach proposed in this paper accounts for the interdependencies among the five objectives considered and demonstrates the role of the optimum SHM planning in service life management of deteriorating structures. The proposed MOPOP SHM planning is applied to the hull structure of a ship subjected to fatigue.

Keywords Damage detection · Fatigue · Maintenance · Probability · Multi-objective optimization · Reliability · Service life · Structural health monitoring

✉ Dan M. Frangopol
dan.frangopol@lehigh.edu

Sunyong Kim
sunyongkim@wku.ac.kr

[1] Department of Civil and Environmental Engineering, Wonkwang Universtiy, 460 Iksandae-ro, Iksan, Jeonbuk 570-749, Republic of Korea

[2] Department of Civil and Environmental Engineering, ATLSS Engineering Research Center, Lehigh University, 117 ATLSS Dr., Bethlehem, PA 18015-4729, USA

1 Introduction

Service life management is essential for a deteriorating structure to ensure its structural safety and extend its service life (Akpan et al. 2002, IAEA 2015, NCHRP 2006). The effectiveness and efficiency of the service life management depend on the accuracy of assessing and predicting the structural performance (Mohanty et al. 2009, NCHRP 2003, Sánchez-Silva et al. 2016). The difficulties encountered in the service life management are largely due to the uncertainties associated with the assessing and predicting processes. Structural health monitoring (SHM) can play an important role in detecting and identifying the damage on time (Chong et al. 2003, Farhey 2006, Liu et al. 2009). If sufficient amount of data can be collected through long-term SHM and the collected data are interpreted rationally, the uncertainties associated with assessing and predicting the structural performance can be reduced. Moreover, the effectiveness and efficiency of service life management can be significantly improved. The integration of the SHM data for service life management of engineering structures has been investigated extensively over the past decade (Frangopol and Soliman 2016).

The integration of the SHM data for service life management helps in reducing the life-cycle cost of a structure (Frangopol and Messervey 2011). This benefit can be maximized through optimizing installation and planning of SHM (Kim and Frangopol 2010). The main objectives of the optimum SHM installation, which determine the locations to be monitored and types of sensors, are to minimize the monitoring costs and maximize the monitoring performance considering the accuracy and reliability of the monitoring data (Chmielewski et al. 2002, Martinez-Luengo et al. 2016, Worden and Burrows 2001). Several approaches for optimum SHM installation with sensing technologies have been developed and applied to aerospace structures, naval ships and bridges (Meo and Zumpano 2005). Only a few studies have been conducted on SHM planning to establish the monitoring schedule. Kim and Frangopol (2010) proposed an approach based on the relationship between the reliability importance of a monitored component and the monitoring cost. Sabatino and Frangopol (2017) proposed an approach considering the risk attitude of a decision maker for optimum SHM planning. However, assessment of damage under uncertainty are not addressed in these investigations.

Recently, the objectives for optimum inspection planning considering assessment of damage, structural performance, service life and life-cycle cost have been developed and applied to multi-objective probabilistic optimization process (MOPOP). Kim and Frangopol (2017) investigated the multi-objective optimum inspection planning for reinforced concrete structures under corrosion, where four objectives are considered simultaneously using an objective reduction approach. However, to the best of authors' knowledge, no studies on probabilistic optimum SHM planning based on a large number of objectives have been reported.

This study proposes a novel approach to establish a multi-objective probabilistic optimum SHM plan for the hull structure of a ship subjected to fatigue. Five probabilistic objectives for optimum SHM planning (i.e. f_1 = minimizing the expected damage detection delay, f_2 = minimizing the expected maintenance delay, f_3 = maximizing the damage detection time-based reliability index, f_4 = maximizing the expected total service life extension, and f_5 = minimizing the expected life-cycle cost) are introduced. The uncertainties associated with initiation and propagation of fatigue damage are considered in the formulations of the damage detection delay. The maintenance delay and reliability index are formulated based on the damage detection delay. Furthermore, the effects of the maintenance actions on the service life and costs for SHM, maintenance and structural failure are integrated in the formulation of the total service life extension and the expected life-cycle cost. The SHM plannings associated with both a single- and a multi-objective probabilistic optimization processes are investigated. From the MOPOP, a set of Pareto optimal solutions providing the number of monitorings, monitoring starting times, and monitoring durations are obtained. The degree of conflict between the initial and reduced objectives is estimated using the dominance relation-based objective reduction approach. Consequently, the essential and redundant objectives are identified. Furthermore, a multiple attribute decision making (MADM) is applied to determine the weights of the essential objectives and select a well-balanced decision alternative associated with the SHM planning. The overall computational flowchart is shown in Fig. 1. The novel approach proposed in this paper accounts for the interdependencies among the damage detection, maintenance, reliability, service life and cost for the optimum SHM planning. Efficient decision making in identifying the essential objectives and selecting a well-balanced solution among the Pareto optimal solutions can be achieved. Furthermore, it is noteworthy that based on the proposed approach, any type of structure under various time-dependent deterioration mechanisms can be considered for optimum SHM planning.

2 Objectives for optimum monitoring planning

The formulation of the objective functions is a significant process wherein the descriptive statements associated with the optimization criterion are converted into mathematical expressions including design variables (Arora 2012). Depending on the type of optimization problem, the objective functions need to be minimized or maximized. In this study, five probabilistic objectives are introduced for optimum SHM planning. Figure 2 shows the schematic for the formulation of the five objectives f_1 to f_5 based on the probabilistic damage assessment. The detailed formulations of the objectives, the associated concepts, and theoretical background are provided in the following sections.

2.1 Damage detection delay

The damage detection delay is formulated considering the uncertainties associated with the damage occurrence/propagation and inspection methods. When N_{ins} inspections are applied, the expected damage detection delay $E(t_{del\_d})$ is expressed as (Kim and Frangopol 2011a, b)

$$E(t_{del\_d}) = \sum_{i=1}^{N_{ins}+1} \left[\int_{t_{ins,i-1}}^{t_{ins,i}} \left\{ t_{del\_d,i} \cdot f_T(t) \right\} dt \right] \quad (1)$$

where $f_T(t)$ is the probability of density function (PDF) of damage occurrence time t, $t_{del\_d,i}$ is the damage detection delay for

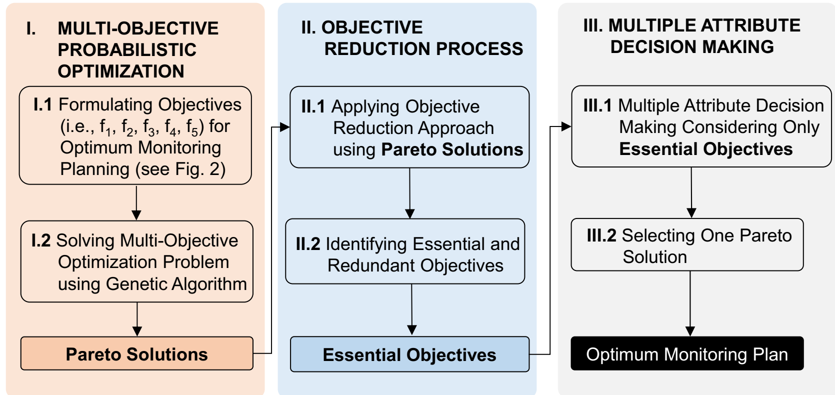

Fig. 1 Computational flowchart for optimum monitoring planning

the damage to occur in the time interval $t_{ins,i-1} \leq t < t_{ins,i}$; and $t_{ins,i}$ is the ith inspection time. If the locations to be monitored and types of sensors are determined properly to maximize the accuracy and reliability of the monitoring data, and there is no damage detection delay during the monitoring duration, $E(t_{del\_d})$ for N_{mon} monitorings can be expressed based on (1) as follows:

$$E(t_{del\_d}) = \sum_{i=1}^{N_{mon}+1} \left[\int_{t_{ms,i-1}+t_{md}}^{t_{ms,i}} (t_{ms,i} - t) \cdot f_T(t) dt \right] \quad (2)$$

where $t_{ms,i}$ = ith monitoring starting time; and t_{md} = monitoring duration. $t_{ms,i-1} + t_{md}$ for $i = 1$ and $t_{ms,i}$ for $i = N_{mon} + 1$ are zero and service life t_{life}, respectively.

2.2 Maintenance delay

The maintenance delay, which is the time interval between the damage occurrence time and the maintenance application time, has to be minimized to improve the maintenance effectiveness. The maintenance delay for a single monitoring (i.e. N_{mon} = 1) is formulated based on the damage detection delay described in (2) with the assumption that the maintenance action is applied for a degree of damage larger than the critical degree as follows:

$$t_{del\_m} = P(a_1 \geq a_{ma}) \times (t_{ms,1} - t) + P(a_1 < a_{ma}) \times (t_{life} - t) \quad \text{for } t \leq t_{ms,1} \quad (3a)$$

$$t_{del\_m} = P(a_1 < a_{ma}) \times (t_{life} - t) \quad \text{for } t_{ms,1} \leq t < t_{ms,1} + t_{md} \quad (3b)$$

$$t_{del\_m} = t_{life} - t \quad \text{for } t_{ms,1} + t_{md} \leq t \quad (3c)$$

where t_{del_m} is the maintenance delay, a_1 is the crack size at time $t_{ms,1} + t_{md}$, and a_{ma} is the critical crack size requiring maintenance actions. Consiering the PDF of the damage occurrence time $f_T(t)$, the expected maintenance delay $E(t_{del\_m})$ can be obtained. Similarly, $E(t_{del\_m})$ for $N_{mon} \geq 2$ can be formulated. When the critical crack size requiring a maintenance action a_{ma} is equal to zero, the expected maintenance delay $E(t_{del\_m})$ is the same as the expected damage detection delay $E(t_{del\_d})$.

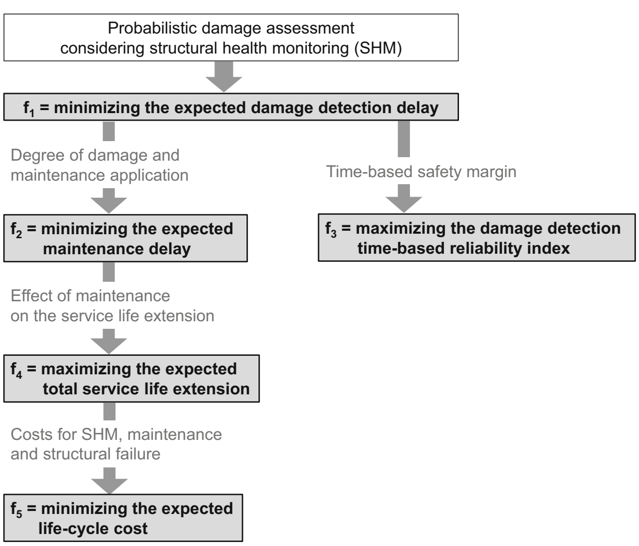

Fig. 2 Formulation of the objectives for optimum SHM planning based on probabilistic damage assessment

2.3 Damage detection time-based reliability index

The reliability index of a deteriorating structure has been used as one of the representative structural performance indicators for service life management of this structure (Frangopol et al. 2011, Frangopol and Soliman 2016). When the damage is not detected, and appropriate and immediate maintenance is not applied before reaching the critical state, a structural failure may occur (Glen et al. 2000, Garbatov and Soares 2014). Considering the relationship between the time-based safety margin t_{mar} and damage detection delay t_{del_d}, the state function $g(\mathbf{T})$ can be expressed as (Kim and Frangopol 2011c)

$$g(\mathbf{T}) = t_{mar} - t_{del\_d} \quad (4)$$

The time-based safety margin t_{mar} is the time interval between the damage occurrence time and the time associated with the critical state. The damage detection delay

t_{del_d} is described in (2). Considering the uncertainties associated with t_{mar} and t_{del_d}, the damage detection time-based probability P_s is expressed as

$$P_s = P(t_{mar} - t_{del\_d} > 0) \quad (5)$$

The damage detection time-based reliability index β is defined as

$$\beta = \Phi^{-1}(P_s) \quad (6)$$

where Φ^{-1} denotes the inverse of the standard normal cumulative distribution function. If damage is not detected until the time associated with the critical state, the time-based safety margin t_{mar} will be equal to or less than t_{del_d}, and the damage detection time-based probability P_s will be zero. The optimum monitoring planning can be based on maximizing the damage detection time-based reliability index β.

2.4 Service life extension

The decision making to apply a maintenance for a deteriorating structure generally depends on the degree of damage detected. The service life management needs to integrate inspection and/or monitoring, and maintenance under uncertainty in a rational way (NCHRP 2012, Soliman et al. 2014, IAEA 2015). Such integration can be addressed in the formulation of the service life extension as follows:

$$t_{exlife} = \sum_{i=1}^{N_{mon}} t_{ex,i} \quad (7)$$

where t_{exlife} is the total service life extension when N_{mon} monitorings are applied. $t_{ex,i}$ is the extension time induced by the maintenance followed by the ith monitoring.

Figure 3 shows the formulation of (7). According to the detected degree of damage (i.e. crack size), the multiple types of maintenance may be determined. Therefore, the service life extension $t_{ex,i}$ in (7) is computed as

$$t_{ex,i} = \sum_{j=1}^{N_{mnt}} P\left(t_{ms,i} + t_{md} \le t_{life,i-1}\right) \cdot P\left(a_{ma,j} \le a_i < a_{ma,j+1}\right) \cdot t^*_{ex,j} \quad (8)$$

where N_{mnt} = number of available maintenance types; $t_{life,i-1}$ = extended service life after the $(i-1)$th monitoring; a_i = crack size at time $t_{ms,i} + t_{md}$; and $t^*_{ex,j}$ = service life extension associated with the jth type of maintenance. The jth type of maintenance action is applied when the crack size a_i is larger than or equal to $a_{ma,j}$, and less than $a_{ma,j+1}$. $t_{life,i-1}$ for $i = 1$ is the initial service life, and $a_{ma,j}$ for $j = N_{mnt} + 1$ is the critical crack size resulting in structural failure a_{crt}. It is important to note that the detectability of damage is assumed to be perfect during monitoring, and the service life can be extended if the ith monitoring is performed before the service life (i.e. $t_{ms,i} + t_{md} \le t_{life,i-1}$) as shown in Fig. 3 and (8). For example, when one monitoring and one type of maintenance are applied (i.e. $N_{mon} = 1$ in (7) and $N_{mnt} = 1$ in (8)), and the service life extension after the maintenance is equal to the initial service life ($t^*_{ex,1} = t_{life,0}$ in (8)), the total service life extension t_{exlife} can be estimated as

$$t_{exlife} = P\left(t_{ms,1} + t_{md} \le t_{life,0}\right) \cdot P\left(a_{ma,1} \le a_1 < a_{crt}\right) \cdot t_{life,0} \quad (9)$$

Furthermore, considering the uncertainty associated with the initial service life, the expected total service life extension $E(t_{exlife})$ can be obtained.

2.5 Life-cycle cost

One of the most representative objectives for service life management is minimizing the expected life-cycle cost (Frangopol and Soliman 2016). The expected life-cycle cost considering SHM C_{lcc} is expressed as (Thoft-Christensen and Sørensen 1987; Frangopol and Messervey 2011)

$$C_{lcc} = C_{mon} + C_{ma} + C_{fail} \quad (10)$$

where C_{mon} = monitoring cost; C_{ma} = in-depth inspection and maintenance cost; and C_{fail} = expected failure cost. The monitoring cost for N_{mon} monitorings is estimated as (Orcesi and Frangopol 2011)

$$C_{mon} = \sum_{i=1}^{N_{mon}} \left(C_{mon,f} + C_{mon,v} \cdot t_{md}\right) \cdot (1 + r_{dis})^{-\left(t_{ms,i} + t_{md}\right)} \quad (11)$$

where $C_{mon,f}$ = fixed cost for preparation and analysis of the monitoring; $C_{mon,v}$ = variable cost depending on the monitoring duration (e.g. operation and maintenance cost); and r_{dis} = discount rate of money. When N_{mnt} maintenance types are available, the formulation of maintenance cost C_{ma} is expressed based on (7) and (8) as follows:

$$C_{ma} = \sum_{i=1}^{N_{mon}} \left(\sum_{j=1}^{N_{mnt}} P\left(t_{ms,i} + t_{md} \le t_{life,i-1}\right) \cdot P\left(a_{ma,j} \le a_i < a_{ma,j+1}\right) \cdot C^*_{ma,j} \cdot (1 + r_{dis})^{-\left(t_{ms,i} + t_{md}\right)} \right) \quad (12)$$

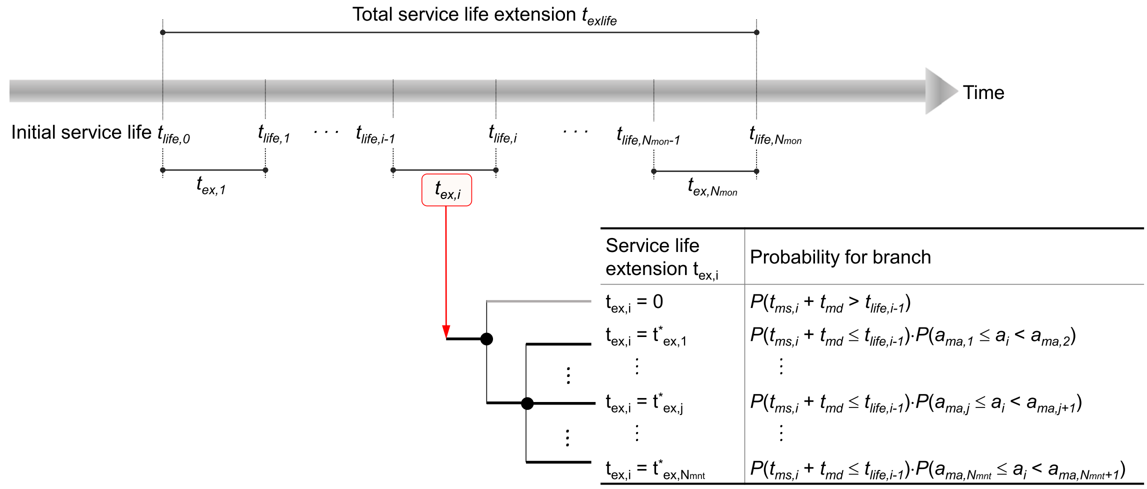

Fig. 3 Formulation of total service life extension

where $C^*_{ma,j}$ = cost associated with the jth maintenance. Furthermore, the expected failure cost C_{fail} in (10) is computed as

$$C_{fail} = P\left(t_{life,i} \le t^*_{life}\right) \cdot C_{lss} \tag{13}$$

where C_{lss} is the expected monetary loss due to the structural failure. The probability of failure is defined as the probability that the service life $t_{life,i}$ is less than the predefined target service life t^*_{life}.

3 Essential and redundant objectives

The Pareto front of the MOPOP is affected by only the essential objectives, and the redundant objectives can be removed without any change in the Pareto front (or Pareto dominance relations). The efficiency of decision making in the MOPOP can be substantially improved by considering only the essential objectives instead of all the objectives. In this study, the dominance relation-based objective reduction approach developed by Brockhoff and Zitzler (2006, 2009) is used to identify the essential and redundant objectives for optimum SHM planning.

Suppose that the initial objective set Ω_I comprises M objectives (i.e., Ω_I: = $\{f_1, f_2,..., f_M\}$) to be minimized in the design space $\mathbf{X}$. A solution $\mathbf{x_1} \in \mathbf{X}$ dominates another solution $\mathbf{x_2} \in \mathbf{X}$ (i.e., $\mathbf{x_1} \prec \mathbf{x_2}$), if and only if $f_i(\mathbf{x_1}) \le f_i(\mathbf{x_2})$ for all objective function of Ω_I, and $f_i(\mathbf{x_1}) < f_i(\mathbf{x_2})$ for at least one objective function of Ω_I. The Pareto optimal solution set Φ_{sol} and Pareto front Φ_{frn} are defined as $\Phi_{sol} := \{\mathbf{x} \in \mathbf{X} \mid \nexists \mathbf{y} \in \mathbf{X} : \mathbf{y} \prec \mathbf{x}\}$ and Φ_{frn}: = $\{\mathbf{z} = (f_1(\mathbf{x}), f_2(\mathbf{x}), \ldots, f_M(\mathbf{x})) \mid \mathbf{x} \in \Phi_{sol}\}$, respectively (Jaimes et al. 2014). Therefore, the Pareto optimal solution set can be represented using the dominance relation. The essential objective set is the smallest set of objectives that can produce the same Φ_{frn} associated with the initial objective set Ω_I. The non-essential objectives among Ω_I are redundant (Saxena et al. 2013).

The degree of conflict δ between the reduced objective set Ω_R and the initial objective set Ω_I is estimated as the maximum difference between the Pareto optimal solutions of Ω_I and those of Ω_R (Brockhoff and Zitzler 2006). Because the objectives may have various units and orders of magnitude for practical application, the degree of conflict δ needs to be normalized. If Ω_R is entirely in conflict with Ω_I, the normalized degree of conflict δ_{norm} is 1.0. The reduced objective set Ω_R associated with $\delta_{norm} = 0$ (i.e., non-conflict) provides Pareto optimal solutions that are identical to the Pareto optimal solutions of Ω_I. It should be noted that the Pareto optimal solutions obtained from the MOPOP of Ω_I are required to identify the essential and redundant objectives through the dominance relation-based objective reduction approach as shown in Fig. 1.

4 Multiple attribute decision making

MADM can be applied to select a well-balanced solution among the Pareto optimal solutions. Based on a simple additive weighting method, the overall assessment value of each Pareto optimal solution is estimated as (Yoon and Hwang 1995)

$$V_i = \sum_{j=1}^{M} w_j z_{ij} \tag{14}$$

where V_i = overall assessment value of the ith solution in the Pareto optimal solution set; z_{ij} = jth normalized objective value associated with the ith Pareto solution; w_j = weight of the jth objective satisfying $w_j \geq 0$ and $\sum_{j=1}^{M} w_j = 1$; and M = number of objectives to be considered in MADM. The best Pareto optimal solution has the largest value of V_i. Overviews on MADM including representative methods and their applications can be found in Yoon and Hwang 1995, Pohekar and Ramachandran 2004, Zavadskas et al. 2014, among others.

The determination of weight w_j in (14) is based on several methods, which can be grouped into subjective, objective and integrated methods (Wang and Luo 2010). The subjective weight determination method depends on the subjective preference of the decision maker. The objective method without the intervention of any decision maker uses decision information including the correlation among the objective values and standard deviation of the objective values. Both the subjective preference of the decision maker and the objective decision information can be considered simultaneously in the integrated method. In this study, the objective weight determination methods such as standard deviation (SD), criteria importance through inter-criteria correlation (CRITIC), and correlation coefficient and standard deviation (CCSD) methods are used.

Based on the SD method, the weight of the jth objective w_j in (14) is determined as (Diakoulaki et al. 1995, Deng et al. 2000)

$$w_j = \frac{\sigma_j}{\sum_{k=1}^{M} \sigma_k} \tag{15}$$

where σ_j = SD of the jth objective values z_j of the Pareto optimal solutions; and M = number of objectives in MADM. The weight of the jth objective w_j in the CRITIC method is estimated as (Diakoulaki et al. 1995)

$$w_j = \frac{\sigma_j \cdot \sum_{k=1}^{M} \left(1 - R_{jk}\right)}{\sum_{k=1}^{M} \left(\sigma_k \cdot \sum_{l=1}^{M} \left(1 - R_{kl}\right)\right)} \tag{16}$$

where R_{kl} = coefficient of correlation between the kth objective values z_k and the lth objective values z_l of the Pareto optimal solutions. Furthermore, in the CCSD method, the weights of the objectives w_j are defined as follows (Wang and Luo 2010).

$$w_j = \frac{\sigma_j \sqrt{1 - R_j}}{\sum_{k=1}^{M} \left(\sigma_k \cdot \sqrt{1 - R_k}\right)} \tag{17}$$

where R_j is the coefficient of correlation between z_j and V_{ij}. V_{ij} is expressed as

$$V_{ij} = \sum_{k=1, k \neq j}^{M} w_j z_{ij} \tag{18}$$

Since the weight of the jth objective w_j is required for computing R_j in (17), w_j needs to be computed using the optimization process as follows:

$$\text{Find } w = \{w_1, \ldots, w_j, \ldots, w_M\} \tag{19a}$$

$$\text{for minimizing } \sum_{j=1}^{M} \left(w_j - \frac{\sigma_j \sqrt{1 - R_j}}{\sum_{k=1}^{M} \left(\sigma_k \cdot \sqrt{1 - R_k}\right)} \right)^2 \tag{19b}$$

$$\text{such that } w_j \geq 0 \text{ and } \sum_{j=1}^{M} w_j = 1 \tag{19c}$$

5 Application to ship hull structures subjected to fatigue

The approach proposed in this paper is applied to a fatigue-sensitive detail of a ship hull structure. The joint between the bottom plate and longitudinal stiffener is considered a fatigue critical location to be monitored in this application. Under longitudinal loading and unloading induced by the hull bottom plate bending, the fatigue crack in the bottom plate can initiate at the joint and propagate away from the longitudinal stiffener. The schematic representation and detailed descriptions including time-dependent crack growth at this location can be found in Kim and Frangopol (2011a). Based on Paris' equation (Paris and Erdogan 1963), the time t for a crack to reach the crack size a_t is expressed as

$$t = \frac{1}{N_{an} \cdot C \cdot S_{re}} \int_{a_0}^{a_t} \left(Y(a) \sqrt{\pi a} \right)^{-m} da \tag{20}$$

where N_{an} is the annual average number of cycles, S_{re} is the equivalent constant-amplitude stress range, a_0 is the initial crack size, and $Y(a)$ is the geometrical correction function. C and m are the material parameter and exponent, respectively. Table 1 lists the values of the deterministic and probabilistic variables required to predict the crack size based on (20). In this study, the geometrical correction function $Y(a)$ is assumed to be one (Madsen et al. 1991, Akpan et al. 2002).

Figure 4 shows the PDFs of the fatigue damage initiation time and time required for the crack to reach the critical crack size using the Monte Carlo simulation with a sample size of 100,000. The criteria for fatigue damage initiation and time required for the crack to reach the critical crack size are assumed 1.0 *mm* and 20 *mm*, respectively. The PDF $f_T(t)$ of the fatigue damage initiation time, as shown in Fig. 4, is used to formulate the expected damage detection delay $E(t_{del\_d})$ and expected maintenance delay $E(t_{del\_m})$. The time required for the crack to reach the critical crack size serves as the initial service life $t_{life,0}$ in the formulations of the state function

Table 1 Variables for fatigue crack size prediction

Random variables	Distribution type	Mean	Coefficient of variation
Annual average number of cycles N_{an}	Lognormal	0.8×10^{6}	0.2
Constant-amplitude stress range S_{re} (MPa)	Weibull	40	0.1
Initial crack size a_0 (mm)	Lognormal	0.5	0.2
Material constant C	Lognormal	3.54×10^{-11}	0.3
Material exponent m	Deterministic	2.54	–

Based on information provided in Kim and Frangopol (2011a)

to estimate the damage detection time-based reliability index β and the total service life extension t_{exlife}.

For steel structures containing fatigue crack damage, several maintenance types can be employed: (a) placing cover plates over the crack; (b) drilling a hole at the end of the crack and fill the hole with a bolt; (c) cutting out and re-fabricating parts of elements; (d) peening; (e) gas tungsten arc remelting, among others (Fisher et al. 1998, Kwon and Frangopol 2011). In this illustrative application, it is assumed that (a) the single maintenance type of cutting out and re-fabricating parts of elements is applied to recover the condition before cracking occurred, when the crack size reaches a_{ma}, and (b) the fatigue crack is detected by using the SHM with strain sensors. Therefore, the service life extension after the maintenance is assumed to be equal to the initial service life ($t^{*}_{ex} = t_{life,0}$ in (8)). Furthermore, the formulation of the expected life-cycle cost considering SHM C_{lcc} is based on the assumptions that the fixed monitoring cost $C_{mon,f}$, variable monitoring cost $C_{mon,v}$, in-depth inspection and maintenance cost C_{ma}, expected failure cost C_{fail} and discount rate of money are \$15,000, \$1000/week, \$65,000, \$1,000,000 and 0, respectively (Soliman et al. 2016). In this paper, the single-objective probabilistic optimization and three types of the MOPOP are investigated for the optimum

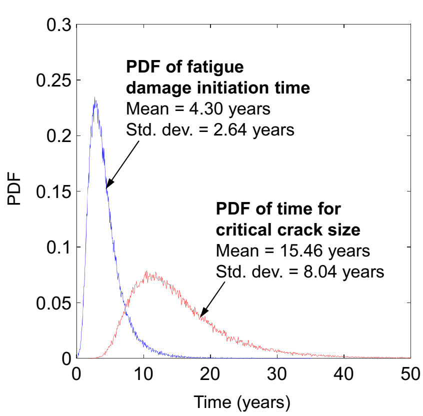

Fig. 4 PDFs of fatigue damage initiation time and time for critical crack size

SHM planning. Type I MOPOP is formulated with the design variables of monitoring starting times $t_{ms,i}$, given monitoring duration t_{md} and number of monitorings N_{mon}. For Type II MOPOP, $t_{ms,i}$ and t_{md} are considered design variables, whereas N_{mon} is given. The design variables of Type III MOPOP are $t_{ms,i}$, t_{md} and N_{mon}.

5.1 Single-objective probabilistic optimization for SHM planning

The single-objective probabilistic optimum SHM planning is obtained as a solution of an optimization problem considering the five objectives f_1 = minimizing the expected damage detection delay $E(t_{del\_d})$ (see (2)), f_2 = minimizing the expected maintenance delay $E(t_{del\_m})$ (see (3)), f_3 = maximizing the damage detection time-based reliability index β (see (6)), f_4 = maximizing the expected total service life extension (see (7)), and f_5 = minimizing the expected life-cycle cost (see (10)), separately. The formulation of the single-objective probabilistic optimization is given as

$$\text{Given } N_{mon} = 2, t_{md} = 0.5 \textit{ year} \tag{21a}$$

$$\text{find } \boldsymbol{t_{ms}} = \left\{t_{ms,1}, t_{ms,2}, \ldots, t_{ms,Nmon}\right\} \tag{21b}$$

$$\text{for } f_1, f_2, f_3, f_4, or\ f_5 \tag{21c}$$

$$\text{such that } 1 \text{ year} \le t_{ms,i} - \left(t_{ms,i-1} + t_{md}\right) < 15 \text{ years} \tag{21d}$$

where $\boldsymbol{t_{ms}}$ = vector of design variables consisting of monitoring starting times $t_{ms,i}$ (years), N_{mon} = number of monitorings, and t_{md} = monitoring duration (years). As indicated in (21d), the non-monitoring time interval has to be larger than 1 year and less than 15 years. This single-objective probabilistic optimization problem is solved using the constrained nonlinear minimization algorithm provided in MATLAB® version R2016b (MathWorks 2016). Figure 5 shows the monitoring plans for the five objectives f_1 to f_5. In order to minimize the expected damage detection delay $E(t_{del\_d})$, the monitoring with t_{md} = 0.5 year has to applied at $t_{ms,1}$ = 4.46 years and $t_{ms,2}$ = 9.86 years, and the associated $E(t_{del\_d})$ is 2.72 years. If

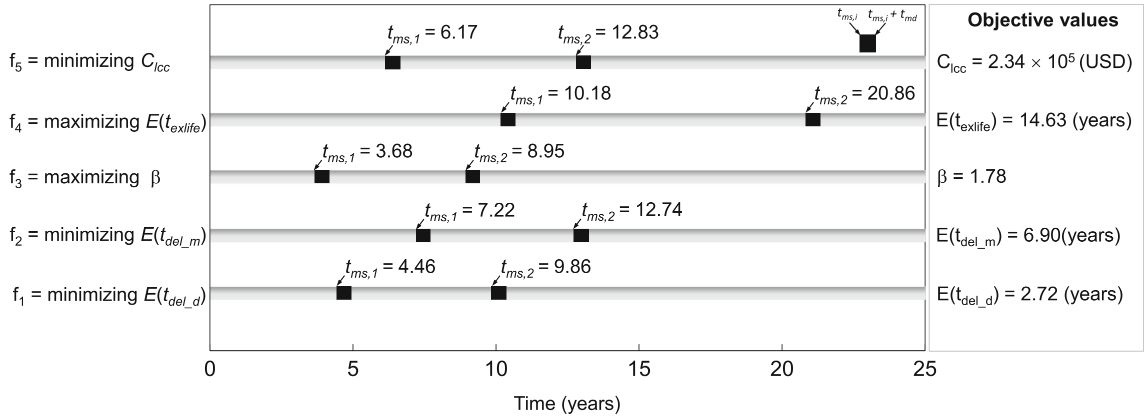

Fig. 5 Monitoring plans based on the single-objective optimization for number of monitorings $N_{mon} = 2$ and monitoring duration $t_{md} = 0.5$ year

the monitoring planning is based on f_2, the monitoring starting times should be 7.22 years and 12.74 years, and $E(t_{del\_m})$ will be 6.90 years.

5.2 Bi-objective probabilistic optimization for SHM planning

Considering f_1 and f_2, the bi-objective probabilistic optimization problem is formulated as

$$\text{Find } \boldsymbol{t_{ms}} = \{t_{ms,1}, t_{ms,2}, \ldots, t_{ms,Nmon}\} \quad (22a)$$

$$\text{for } f_1 \text{ and } f_2 \quad (22b)$$

The design variables are the monitoring starting times $\boldsymbol{t_{ms}}$. The given conditions and constraints are identical with those in (21a) and (21d). This bi-objective probabilistic optimization problem comes under Type I MOPOP. The Pareto solutions of the bi-objective probabilistic optimization problem are obtained after 500 generations with 100 populations using the genetic algorithms of MATLAB® version R2016b (MathWorks 2016). It should be noted that any combination of two objectives from f_1 to f_6 can be applied for the bi-objective probabilistic optimization problem.

The interdependence between the objective functions can be represented by the correlation coefficient ranging from −1.0 to +1.0. In general, two types of coefficients of correlation (i.e. Pearson's and Spearman's coefficients of correlation) are used. The Pearson's correlation coefficient $R_{p,cor}$ is used to measure the degree of the linear relationship between the two functions f_i and f_j as follows:

$$R_{p,cor} = \frac{E\left[\{f_i(\mathbf{x})-\mu_i\}\cdot\{f_j(\mathbf{x})-\mu_j\}\right]}{\sigma_i\cdot\sigma_j} \quad (23)$$

where $\boldsymbol{x}$ is the vector of the design variables in the design space, and μ_i and σ_i are the mean and standard deviation of the objective function f_i values, respectively. Spearman's coefficient of correlation $R_{s,cor}$ is a measure of a monotone association between two the objective functions f_i and f_j. $R_{s,cor}$ is computed as (Myers et al. 2003, Hauke and Kossowski 2011)

$$R_{s,cor} = 1-\frac{6\sum_{i=1}^{n} d_i^2}{n(n^2-1)} \quad (24)$$

where n = number of values of each objective in the design space; and d_i = difference between the ranks of values of the objective functions f_i and f_j.

Figure 6 illustrates the relation between $E(t_{del\_d})$ and $E(t_{del\_m})$ in the criterion space, and the Pareto solutions

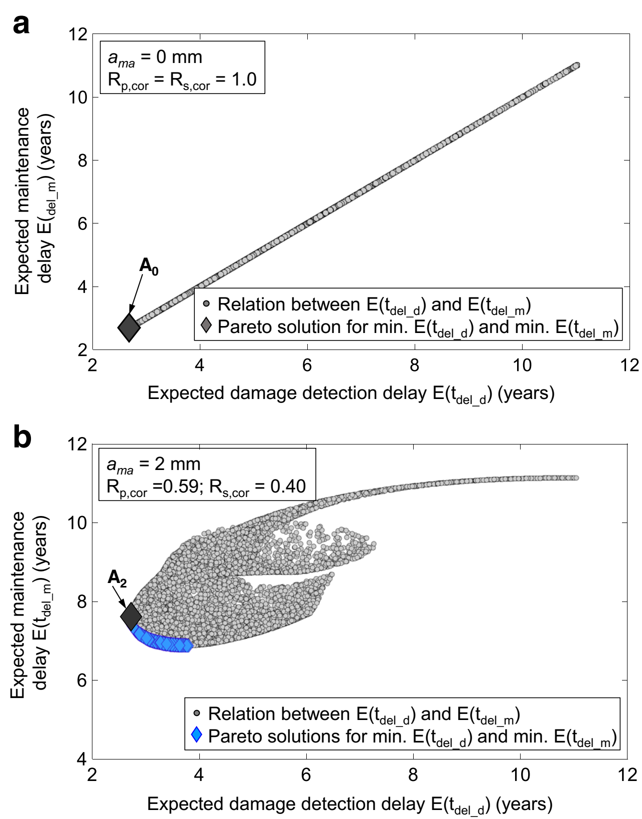

Fig. 6 Relation between expected damage detection delay and expected maintenance delay in the criterion space and the associated Pareto solutions: **a** $a_{ma} = 0$ mm; **b** $a_{ma} = 2$ mm

Table 2 Objective function values associated with Pareto optimum solutions in Figs. 6, 9, 10, and 11

Pareto optimum solution	Expected damage detection delay $E(t_{del\_d})$ (years)	Expected maintenance delay $E(t_{del\_m})$ (years)	Damage detection time-based reliability index β	Expected total service life extension $E(t_{exlife})$ (years)	Expected life-cycle cost C_{lcc} (USD)
A_0	2.72	2.72	–	–	–
A_2	2.72	7.61	–	–	–
$B_{SD} = B_{CR} = B_{CS}$	–	7.08	1.43	11.29	233,560.16
$C_{SD} = C_{CS}$	–	–	1.05	5.58	413,444.45
C_{CR}	–	–	1.21	4.98	548,028.90
C_{AV}	–	–	1.07	5.54	421,749.67
$D_{SD} = D_{CR} = D_{AV}$	–	5.72	1.71	11.07	392,871.77
D_{CS}	–	5.96	1.71	11.52	392,586.81
$E_{SD} = E_{CR} = E_{CS} = E_{AV}$	–	5.30	1.62	18.11	490,051.67
$F_{SD} = F_{CR} = F_{CS} = F_{AV}$	–	5.30	1.62	18.11	490,051.67

associated with the bi-objective probabilistic optimization problem of (22a and 22b). If the critical crack size requiring maintenance action a_{ma} is zero, the maintenance is applied immediately when the damage is detected, and as a result the expected maintenance delay $E(t_{del\_m})$ will be the same as the expected damage detection delay $E(t_{del\_d})$. Moreover, the Pearson's and Spearman's coefficients of correlation between $E(t_{del\_d})$ and $E(t_{del\_m})$ are both equal to one (i.e. $R_{p,cor} = R_{s,cor} = 1.0$), and only one Pareto optimal solution exists as shown in Fig. 6a. For this reason, $E(t_{del\_d})$ or $E(t_{del\_m})$ can be ignored in the MOPOP.

When the critical crack size requiring maintenance action $a_{ma} = 2$ *mm* is considered, $E(t_{del\_d})$ and $E(t_{del\_m})$ become partially correlated (i.e. $R_{p,cor} = 0.59$ and $R_{s,cor} = 0.40$), and multiple Pareto optimal solutions exists as shown in Fig. 6b. The objective values of $E(t_{del\_d})$ and $E(t_{del\_m})$ associated with the representative solutions A_0 and A_2 in Fig. 6 are presented in Table 2. Table 3 provides the values of the design variable (i.e. monitoring starting times $t_{ms,1}$ and $t_{ms,2}$) and given conditions ($t_{md} = 0.5$ year, $N_{mon} = 2$) for A_0 and A_2. The SHM plan for solution A_0 requires two monitorings at $t_{ms,1} = 4.46$ years and $t_{ms,2} = 9.86$ years with a monitoring duration t_{md} of 0.5 year (see Table 3). $E(t_{del\_d})$ and $E(t_{del\_m})$ are equal to 2.72 years as indicated in Table 2. It is important to note that the SHM plans corresponding to the two solutions A_0 and A_2, and the solution of the single objective optimization problem with f_1 are identical as shown in Fig. 5 and Table 3.

5.3 Type I MOPOP for optimum SHM planning

The initial objective set Ω_I consisting of the five objectives f_1, f_2, f_3, f_4 and f_5 are considered simultaneously for the MOPOP formulation as follows:

Table 3 Values of design variables and given conditions associated with Pareto optimum solutions in Figs. 6, 9, 10, and 11

Pareto optimum solution	Design variables or given conditions							Type of MOPOP
	Optimum monitoring starting times (years)			Monitoring durations (years)			Number of monitorings N_{mon}	
	$t_{ms,1}$	$t_{ms,2}$	$t_{ms,3}$	$t_{md,1}$	$t_{md,2}$	$t_{md,3}$		
A_0	4.46	9.86	–	0.5*	0.5*	–	2*	I
A_2	4.46	9.86	–	0.5*	0.5*	–	2*	I
$B_{SD} = B_{CR} = B_{CS}$	6.17	12.83	–	0.5*	0.5*	–	2*	I
$C_{SD} = C_{CS}$	7.98	–	–	2.0	–	–	1*	II
C_{CR}	6.95	–	–	2.0	–	–	1*	II
C_{AV}	7.90	–	–	2.0	–	–	1*	II
$D_{SD} = D_{CR} = D_{AV}$	4.70	11.23	–	1.97	1.98	–	2*	II
D_{CS}	4.74	12.29	–	1.98	1.53	–	2*	II
$E_{SD} = E_{CR} = E_{CS} = E_{AV}$	4.91	11.46	21.44	1.61	1.71	1.56	3*	II
$F_{SD} = F_{CR} = F_{CS} = F_{AV}$	4.91	11.46	21.44	1.61	1.71	1.56	3	III

* Given conditions

Table 4 Normalized degree of conflict δ_{norm} between the initial objective set Ω_I and the representative reduced objective set Ω_R

Type of MOPOP	Number of monitorings $N_{mon} = 1$		Number of monitorings $N_{mon} = 2$		Number of monitorings $N_{mon} = 3$	
	Ω_R	δ_{norm}	Ω_R	δ_{norm}	Ω_R	δ_{norm}
I	$\{f_1, f_4\}$	0.219	$\{f_1, f_4\}$	0.620	$\{f_1, f_4\}$	0.952
	$\{f_2, f_3, f_4\}$	0.0	$\{f_2, f_3, f_4\}$	0.113	$\{f_2, f_3, f_4\}$	0.915
	$\{f_2, f_3, f_4, f_5\}$	0.0	$\{f_2, f_3, f_4, f_5\}$	0.002	$\{f_2, f_3, f_4, f_5\}$	0.002
II	$\{f_3, f_4\}$	0.345	$\{f_3, f_4\}$	0.856	$\{f_3, f_4\}$	1.0
	$\{f_3, f_4, f_5\}$	0.0	$\{f_3, f_4, f_5\}$	0.759	$\{f_3, f_4, f_5\}$	0.622
	$\{f_2, f_3, f_4, f_5\}$	0.0	$\{f_2, f_3, f_4, f_5\}$	0.0	$\{f_2, f_3, f_4, f_5\}$	0.0
III	$\{f_2, f_4\}$	1.0	Note: Number of monitorings N_{mon} is a design variable for Type III MOPOP.			
	$\{f_2, f_4, f_5\}$	0.478				
	$\{f_2, f_3, f_4, f_5\}$	0				

$$\text{Given } N_{mon}, t_{md} \tag{25a}$$

$$\text{find } t_{ms} = \{t_{ms,1}, t_{ms,2}, \ldots, t_{ms,Nmon}\} \tag{25b}$$

$$\text{for } \Omega_I = \{f_1, f_2, f_3, f_4, f_5\} \tag{25c}$$

$$\text{such that } 1\ year \le t_{ms,i} - (t_{ms,i-1} + t_{md}) < 15\ years \tag{25d}$$

As indicated in (25a and 25d), the design variables of the MOPOP are the monitoring starting times $\boldsymbol{t_{ms}}$, and the monitoring duration and number of monitorings are given (i.e. t_{md} = 0.5 year, and N_{mon} = 1, 2, or 3). This formulation is associated with Type I MOPOP. For Type I, II and II MOPOPs in this study, the critical crack size requiring maintenance action a_{ma} = 2 mm is applied, and the Pareto solution set is computed by using the genetic algorithms of MATLAB® version R2016b (MathWorks 2016) after 500 generations with 300 populations. In order to assess the degree of conflict between the initial objective set Ω_I and the reduced objective set Ω_R, and to identify the essential objectives, the dominance relation-based objective reduction approach is applied with the computed Pareto solution set.

Table 4 presents the normalized degree of conflict δ_{norm} between Ω_I and Ω_R. For N_{mon} = 1, the values of δ_{norm} associated with the reduced objective sets $\{f_1, f_4\}$, $\{f_2, f_3, f_4\}$, and $\{f_2, f_3, f_4, f_5\}$ are 0.219, 0.0 and 0.0, respectively. Figure 7 shows the comparison between the Pareto solutions of the objective sets $\Omega_I = \{f_1, f_2, f_3, f_4, f_5\}$ and $\Omega_R = \{f_2, f_3, f_4\}$ in the 3D Cartesian coordinate system, which consists of $E(t_{del\_m})$, β and $E(t_{exlife})$ as shown in Fig. 7. The Pareto solutions of Ω_I with five dimensions (equal to the number of objectives to be considered) are projected onto this 3D Cartesian coordinate systems. The Pareto front of $\Omega_I = \{f_1, f_2, f_3, f_4, f_5\}$ is the same as the Pareto front of $\Omega_R = \{f_2, f_3, f_4\}$ because the associated δ_{norm} is equal to zero. Hence, $\Omega_R = \{f_2, f_3, f_4\}$ is the essential objective set, and f_1 and f_5 are redundant.

For N_{mon} = 2, δ_{norm} between Ω_I and $\Omega_R = \{f_2, f_3, f_4, f_5\}$ is 0.002 as indicated in Table 4. Figure 8 compares the Pareto solution sets of Ω_I and $\Omega_R = \{f_2, f_3, f_4, f_5\}$ in the 3D Cartesian coordinate system. Because the dimension of the Pareto solutions for $\Omega_R = \{f_2, f_3, f_4, f_5\}$ is equal to the number of objectives to be considered (i.e. four), the Pareto solutions are illustrated in the four 3D Cartesian coordinate systems as shown in Fig. 8. Figure 9 illustrates the Pareto optimal solutions for the essential objective set $\{f_2, f_3, f_4, f_5\}$ in the parallel coordinate system, where the four vertical axes represent the values of $E(t_{del\_d})$, β, $E(t_{exlife})$ and C_{lcc}. When an allowable normalized degree of conflict δ_{all} of 0.002 is applied, the essential objective set becomes $\{f_2, f_3, f_4, f_5\}$. For this reason, the redundant objective f_1 is ignored in the MADM for selecting the well-balanced Pareto optimal solutions. The weights of the essential objectives f_2, f_3, f_4 and f_5 are computed using the SD (see (15)), CRITIC (see (16)) and CCSD (see (17)) methods. The overall assessment values of the Pareto solutions for $\{f_2, f_3, f_4, f_5\}$ are estimated using the simple additive weight method defined in (14). It should be noted that even though there are

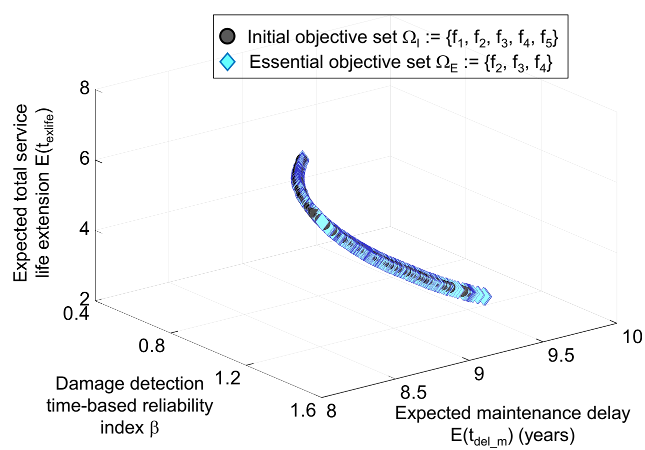

Fig. 7 Pareto solutions of the initial objective and essential objective sets of Type I MOPOP for N_{mon} = 1

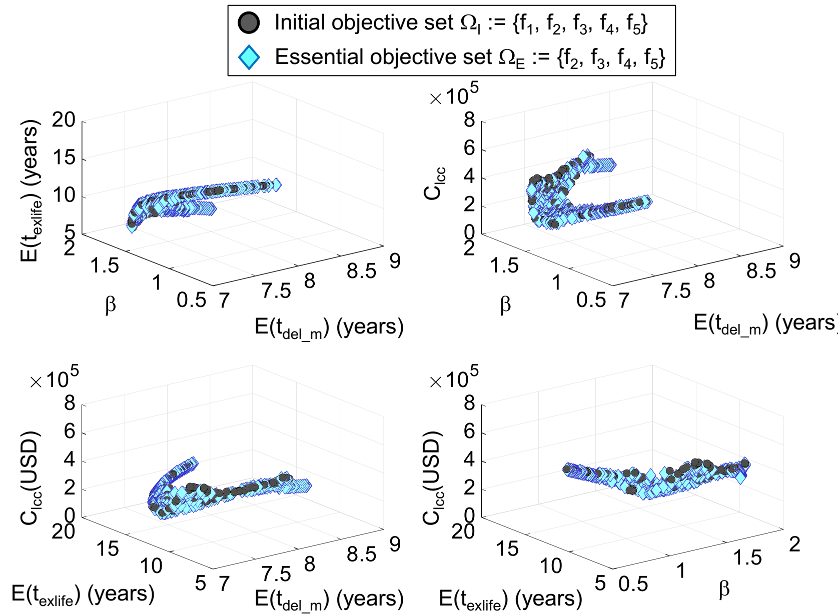

Fig. 8 Pareto solutions of the initial objective and essential objective sets $\Omega_E = \{f_2, f_3, f_4, f_5\}$ of Type I MOPOP for $N_{mon} = 2$ in the 3D Cartesian coordinate system

the Pareto solutions from the bi-objective optimization with only the objectives f_1 and f_2 (see Fig. 6b), the objective f_1 can be redundant in Type I MOPOP considering the objectives f_1, f_2, f_3, f_4 and f_5 simultaneously.

The solutions B_{SD}, B_{CR} and B_{CS}, as shown in Fig. 9, are associated with the largest overall assessment values based on the SD, CRITIC and CCSD methods, respectively. The values of the objectives and design variables for B_{SD}, B_{CR} and B_{CS} are provided in Tables 2 and 3. The three solutions B_{SD}, B_{CR} and B_{CS} lead to the same monitoring plan, which requires two monitorings at 6.17 years and 12.83 years (see Table 3). The associated $E(t_{del\_m})$, β, $E(t_{exlife})$ and C_{lcc} are 7.08 years, 1.43, 11.29 years and \$233,560.16, respectively, as indicated in Fig. 9 and Table 2.

5.4 Type II MOPOP for optimum SHM planning

The Type II MOPOP considering the monitoring starting times $t_{ms,i}$ and monitoring durations $t_{md,i}$ as design variables is formulated as

$$\text{Given } N_{mon} \tag{26a}$$

$$\text{find } t_{ms} = \{t_{ms,1}, t_{ms,2}, \ldots, t_{ms,Nmon}\} \text{ and } t_{md} = \{t_{md,1}, t_{md,2}, \ldots, t_{md,Nmon}\} \tag{26b}$$

$$\text{for } \Omega_I = \{f_1, f_2, f_3, f_4, f_5\} \tag{26c}$$

$$\text{such that } 1\ year \le t_{ms,i} - (t_{ms,i-1} + t_{md,i}) < 15\ years \text{ and } t_{md,i} \le 2\ years \tag{26d}$$

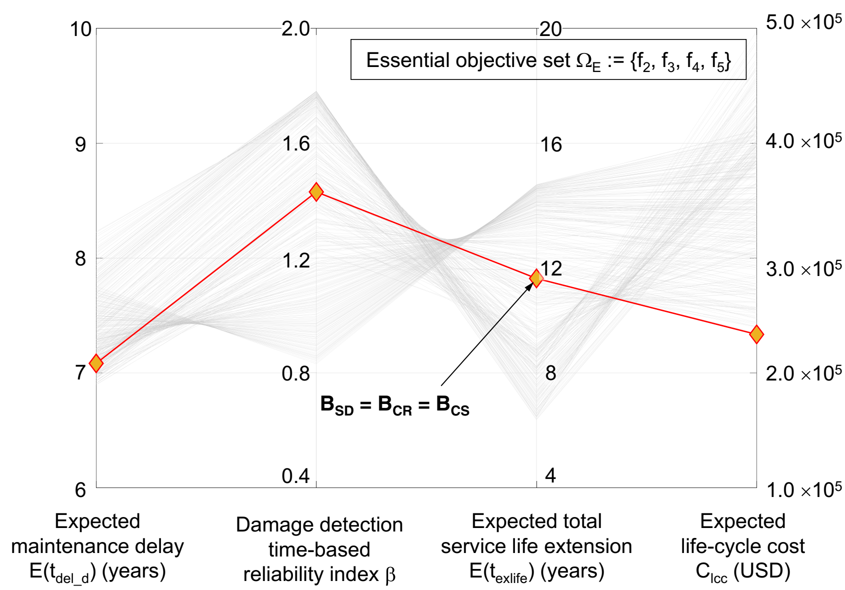

Fig. 9 Multi-attribute decision alternatives for the essential objective set $\Omega_E = \{f_2, f_3, f_4, f_5\}$ of Type I MOPOP for $N_{mon} = 2$ in the parallel coordinate system

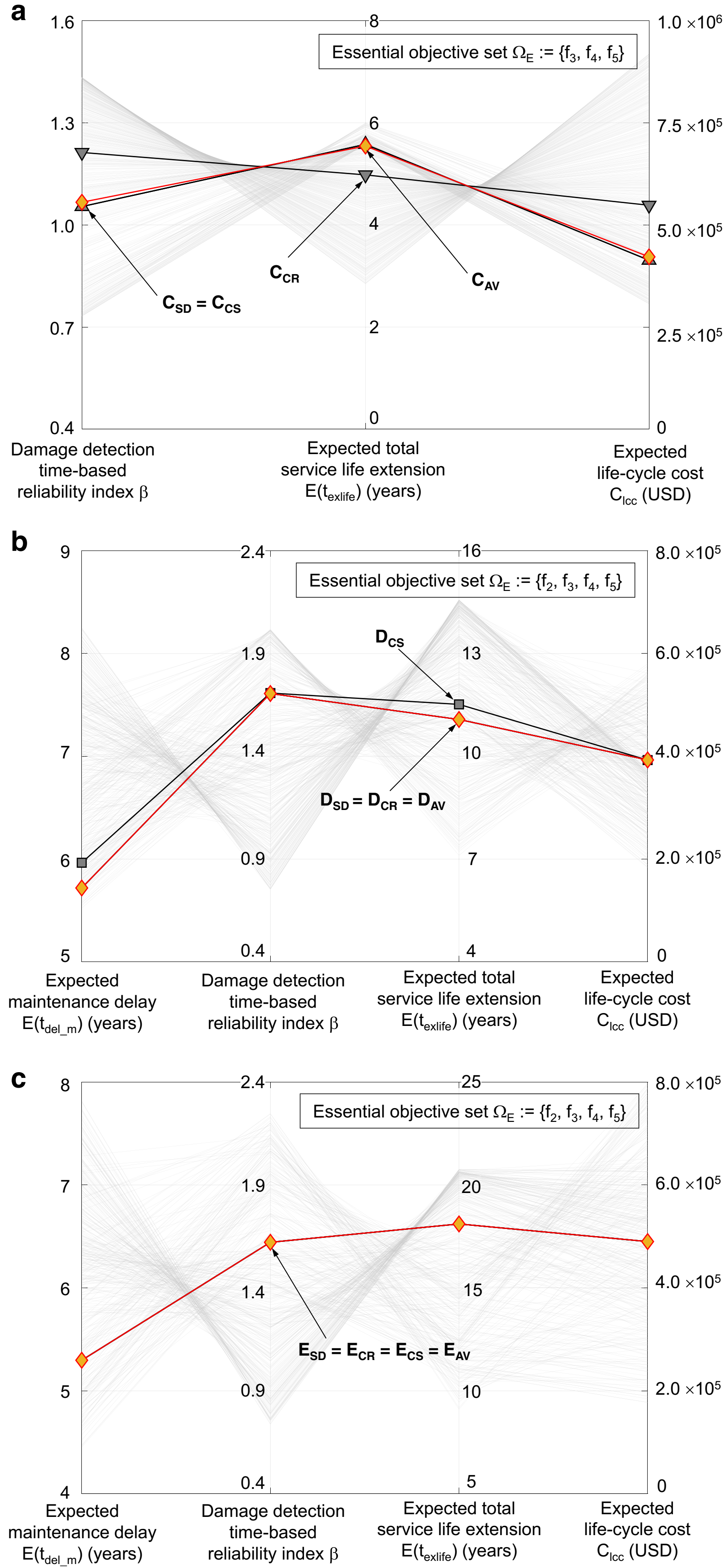

Fig. 10 Multi-attribute decision alternatives of the Pareto optimal solutions of Type II MOPOP in the parallel coordinate system: **a** N_{mon} = 1; **b** N_{mon} = 2; **c** N_{mon} = 3

Fig. 11 Multi-attribute decision alternative of the Pareto optimal solutions of Type III MOPOP in the parallel coordinate system

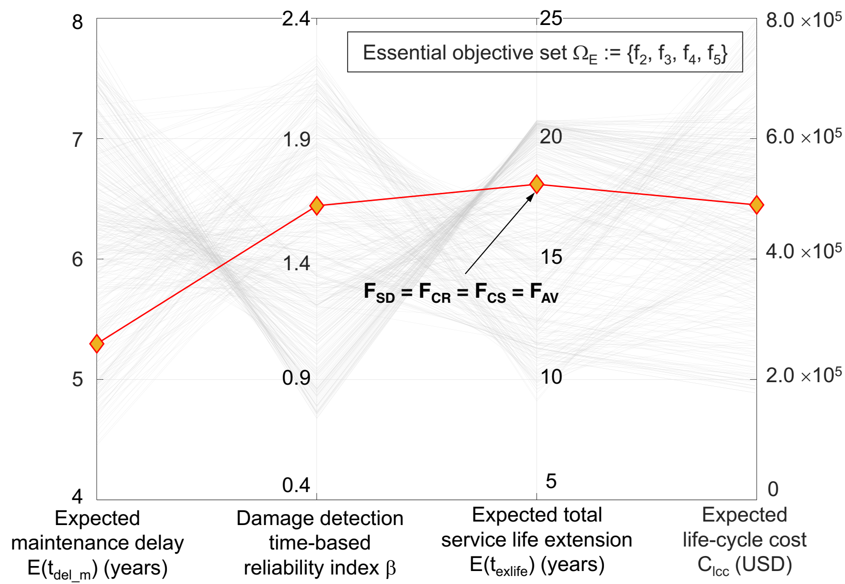

As presented in (26d), the non-monitoring time interval should be between 1 year and 15 years, and the monitoring duration has to be less than 2 years. Table 4 presents the normalized degree of conflict δ_{norm} between Ω_I and the representative reduced objective set Ω_R. The essential objective sets for N_{mon} = 1, 2 and 3 are $\{f_3, f_4, f_5\}$, $\{f_2, f_3, f_4, f_5\}$, and $\{f_2, f_3, f_4, f_5\}$, respectively. The computed Pareto solutions of the essential objective sets for N_{mon} = 1, 2 and 3 are presented in the parallel coordinate system as shown in Fig. 10. For N_{mon} = 1, the representative Pareto solutions C_{SD}, C_{CR} and C_{CS} in Fig. 10a are selected using the SD, CRITIC and CCSD methods. In order to consider the weights of the objectives estimated by the SD, CRITIC and CCSD methods simultaneously, the average weights of the objectives are calculated as

$$w_j = \frac{(w_{j,SD} + w_{j,CR} + w_{j,CS})}{3} \quad (27)$$

where $w_{j,SD}$, $w_{j,CR}$ and $w_{j,CS}$ are the weights of the jth objective obtained using the SD, CRITIC and CCSD methods, respectively. The selection of the solution C_{AV} shown in Fig. 10a is based on the average weights defined in (27). As presented in Table 2 and Fig. 10, the solution C_{SD} is identical to C_{CS}, and the objective values of the solution C_{AV} are close to those of the solution C_{SD} (or C_{CS}). Figure 10b shows the Pareto solutions and the selected solutions D_{SD} (equal to D_{CR} and D_{AV}) and D_{CS} when N_{mon} = 2. Furthermore, Fig. 10c and Tables 2 and 3 indicate that the selected solutions based on the SD CRITIC and CCSD methods are the same (i.e. $E_{SD} = E_{CR} = E_{CS}$). Thus, the solution E_{AV} is the same as the other solutions E_{SD}, E_{CR} and E_{CS}. These solutions leads to three monitorings at 4.91 years, 11.46 years and 21.44 years (see Table 3).

5.5 Type III MOPOP for optimum SHM planning

The formulation of Type III MOPOP is

$$\text{Find } t_{ms} = \{t_{ms,1}, t_{ms,2}, \ldots, t_{ms,Nmon}\}, t_{md} = \{t_{md,1}, t_{md,2}, \ldots, t_{md,Nmon}\} \text{ and } N_{mon} \quad (28a)$$

$$\text{for } \Omega_I = \{f_1, f_2, f_3, f_4, f_5\} \quad (28b)$$

The design variables of Type III MOPOP are the monitoring starting times, monitoring duration and number of monitorings. The identical constraints of (26d) are applied in this MOPOP. The Pareto solutions of this MOPOP are obtained by estimating the dominance relations among the Pareto solutions for N_{mon} = 1, 2 and 3 obtained from Type II MOPOP. As indicated in Table 4, the essential objective set for δ_{norm} = 0.0 is $\{f_2, f_3, f_4, f_5\}$. The Pareto solutions for $\{f_2, f_3, f_4, f_5\}$ are illustrated in the parallel coordinate system as shown in Fig. 11. The solutions F_{SD}, F_{CR} and F_{CS} are obtained using the SD, CRITIC, and CCSD methods, respectively. These solutions are identical; moreover, the solution F_{AV} based on the average weights is the same (see Fig. 11, and Tables 2 and 3). It is important to note that the solutions F_{SD}, F_{CR} and F_{CS} shown in Fig. 11 results in the same monitoring plan when the solutions E_{SD}, E_{CR} and E_{CS} in Fig. 10c are applied (see Tables 2 and 3).

6 Conclusions

In this study, a novel approach is proposed to establish the MOPOP SHM plan. The Pareto solutions obtained from the MOPOP are used to identify the redundant objectives using the dominance relation-based objective reduction approach. MADM is applied to determine the weights of the essential objectives, and select a well-balanced solution among the Pareto solution set for the SHM planning. The following conclusions can be drawn:

(1) The proposed five objectives for optimum SHM planning are formulated based on the fatigue damage assessment. To formulate the objective functions of the expected damage detection delay, expected maintenance delay, and damage detection time-based reliability index, the damage occurrence / propagation under uncertainty needs to be estimated. The effect of maintenance on the service life extension is addressed in the formulation of the total service life extension. Furthermore, costs related to monitoring, maintenance and failure are integrated into the total life-cycle cost. The single objective probabilistic optimization based on each individual objective function can lead to its own optimum SHM plan.

(2) The interdependence between the damage detection delay and maintenance delay depends on the critical fatigue crack for maintenance. If the critical fatigue crack is predefined as zero, the maintenance delay is perfectly correlated with the damage detection delay, and a single optimum solution from the bi-objective probabilistic optimization is obtained by minimizing the expected damage detection delay and expected maintenance delay. If the critical fatigue damage for maintenance action is larger than zero, the damage detection delay and maintenance delay become partially correlated, and thus multiple optimum solutions (i.e. Pareto solutions) of the bi-objective optimization exist.

(3) The four-objective set comprising f_2, f_3, f_4, and f_5 is associated with a normalized degree of conflict approximately equal to zero for all the three types of MOPOP. The objective f_1 is redundant and ignored in the MADM. This is because f_1 is highly and positively correlated with f_2, f_3, f_4 and f_5 as shown in Fig. 2.

(4) In this paper, the weights of only the essential objectives are considered in improving the efficiency and effectiveness of the MADM. This is because the redundant objectives do not affect the Pareto front. Furthermore, depending on the type of the weight determination approach to be applied, the weights of the objectives can be varied, and as a result, the selection of a well-balanced solution among the Pareto solution may not be consistent. For a more rational selection of the Pareto solution, the average weights obtained from the multiple weight determination approaches can be used.

(5) The formulations of the objectives presented in this paper are based on the assumption that existing structural damage is detected during the monitoring period. Further studies are needed to address the uncertainty associated with damage detection during monitoring by considering false information, and inappropriate interpretation of information.

(6) The uncertainties associated with the damage propagation and the maintenance effect on the service life extension and life-cycle cost can affect the Pareto solutions of the MOPOP, and selection of the well-balanced Pareto solution in the MADM. Through the appropriate updating process, the accuracy of the probabilistic variables, fatigue crack propagation model, and the optimum SHM planning can be improved.

(7) Increase of the number of objectives leads to a higher computational cost and lower ability to search the Pareto front. For this reason, when the MOPOP with a larger number of objectives is solved, the applicability of an algorithm needs to be evaluated considering both its efficiency and accuracy.

Acknowledgements The support by grants from (a) the National Science Foundation (NSF) Award CMMI-1537926, (b) the Commonwealth of Pennsylvania, Department of Community and Economic Development, through the Pennsylvania Infrastructure Technology Alliance (PITA), (c) the U.S. Federal Highway Administration (FHWA) Cooperative Agreement Award DTFH61-07-H-00040, (d) the U.S. Office of Naval Research (ONR) Awards N00014-08-1-0188, N00014-12-1-0023, and N00014-16-1-2299, (e) the National Aeronautics and Space Administration (NASA) Award NNX10AJ20G, and (f) the Regional Development Research Program by Ministry of Land, Infrastructure and Transport of Korean government Award 16RDRP-B076564-03 is gratefully acknowledged. The opinions presented in this paper are those of the authors and do not necessarily reflect the views of the sponsoring organizations.

Notations β, Damage detection time-based reliability index; δ, Degree of conflict between Ω_R and Ω_I; δ_{norm}, Normalized degree of conflict between Ω_R and Ω_I; a_0, Initial crack size; a_{crt}, Critical crack size resulting in structural failure; a_{ma}, Critical crack size requiring maintenance action; C_{fail}, Expected failure cost; C_{lcc}, Expected life-cycle cost; C_{lss}, Expected monetary loss due to the structural failure; C_{ma}, In-depth inspection and maintenance cost; C_{mon}, Monitoring cost; $E(t_{del\_d})$, Expected damage detection delay; $E(t_{del\_m})$, Expected maintenance delay; f_1, Minimizing the expected damage detection delay; f_2, Minimizing the expected maintenance delay; f_3, Maximizing the damage detection time-based reliability index; f_4, Maximizing the expected total service life extension; f_5, Minimizing the expected life-cycle cost; N_{mnt}, Number of available maintenance types; N_{mon}, Number of monitorings; t_{del_d}, Damage detection delay; t_{del_m}, Maintenance delay; $t_{ex,i}$, Service life extension induced by the maintenance followed by the *i*th monitoring; t_{exlife}, Total service life extension; $t_{ins,i}$, *i*th inspection time; $t_{life,i}$, Extended service life after the *i*th monitoring; t_{ma}, Time interval between the damage occurrence time and the time associated with the critical state; t_{md}, Monitoring duration; t_{ms}, Monitoring starting time; w_i, Weight of the *i*th objective; Ω_I, Initial objective set; Ω_R, Reduced objective set; Φ_{frn}, Pareto front; Φ_{sol}, Pareto optimal solution set

References

Akpan UO, Koko TS, Ayyub B, Dunbar TE (2002) Risk assessment of aging ship hull structures in the presence of corrosion and fatigue. Mar Struct Elsevier 15(3):211–231

Arora JS (2012) Introduction to optimum design, 3rd edn. Elsevier, UK

Brockhoff D, Zitzler E (2006) Dimensionality reduction in multiobjective optimization with (partial) dominance structure preservation: Generalized minimum objective subset problems. TIK Report 247, ETH Zurich, Switzerland

Brockhoff D, Zitzler E (2009) Objective reduction in evolutionary multiobjective optimization: theory and applications. Evol Comput MIT Press 17(2):135–166

Chmielewski DJ, Palmer T, Manousiouthakis V (2002) On the theory of optimal sensor placement. AICHE J 48(5):1001–1012

Chong KP, Carino NJ, Washer G (2003) Health monitoring of civil infrastructures. Smart Mater Struct Institute of Physics Publishing 12(3): 483–493

Deng H, Yeh C-H, Willis RJ (2000) Inter-company comparison using modified TOPSIS with objective weights. Comput Oper Res Pergamon 27(10):963–973

Diakoulaki D, Mavrotas G, Papayannakis L (1995) Determining objective weights in multiple criteria problems: the critic method. Comput Oper Res Pergamon 22(7):763–770

Farhey DN (2006) Instrumentation system performance for long-term bridge health monitoring. Struct Health Monit 5(2):143–153 SAGE

Fisher JW, Kulak GL, Smith IF (1998) A fatigue primer for structural engineers. National Steel Bridge Alliance, Chicago

Frangopol DM, Messervey TB (2011) Effect of monitoring on reliability of structures. In: Bakht B, Mufti AA, Wegner LD (eds) Chapter 18 in monitoring Technologies for Bridge Management. Multi-Science Publishing Co. Ltd., U.K., pp 515–560

Frangopol DM, Soliman M (2016) Life-cycle of structural systems: recent achievements and future directions. Struct Infrastruct Eng 12(1):1–20 Taylor & Francis

Frangopol DM, Saydam D, Kim S (2011) Maintenance, management, life-cycle design and performance of structures and infrastructures: a brief review. Struct Infrastruct Eng Taylor & Francis 8(1):1–25

Garbatov Y, Soares CG (2014) Risk-based Maintenance of Aging Ship Structures. Maintenance and Safety of Aging Infrastructure: Structures and Infrastructures Book Series, 10, 307

Glen LF, Dinovitzer A, Malik L, Basu R, Yee R (2000) Guide to damage tolerance analysis of marine structures. Rep. No. SSC-409, Ship Structure Committee, Washington, DC

Hauke J, Kossowski T (2011) Comparison of values of pearson's and spearman's correlation coefficients on the same sets of data. Quaestiones Geographicae 30(2):87–93

IAEA (2015) Plant Life Management Models for Long Term Operation of Nuclear Power Plants. IAEA Nuclear Energy Series No. NP-T-3.18, International Atomic Energy Agency, Vienna

Jaimes LA, Coello CAC, Aguirre H, Tanaka K (2014) Objective space partitioning using conflict information for solving many-objective problems. Inf Sci Elsevier 268:305–327

Kim S, Frangopol DM (2010) Optimal planning of structural performance monitoring based on reliability importance assessment. Probab Eng Mech Elsevier 25(1):86–98

Kim S, Frangopol DM (2011a) Optimum inspection planning for minimizing fatigue damage detection delay of ship hull structures. Int J Fatigue Elsevier 33(3):448–459

Kim S, Frangopol DM (2011b) Inspection and monitoring planning for RC structures based on minimization of expected damage detection delay. Probab Eng Mech Elsevier 26(2):308–320

Kim S, Frangopol DM (2011c) Cost-based optimum scheduling of inspection and monitoring for fatigue sensitive structures under uncertainty. J Struct Eng ASCE 137(11):1319–1331

Kim S, Frangopol DM (2017) Efficient multi-objective optimisation of probabilistic service life management. Struct Infrastruct Eng Talyor & Francis 13(1):147–159

Kwon K, Frangopol, DM (2011). "Bridge fatigue assessment and management using reliability-based crack growth and probability of detection models." Probab Eng Mech, Elsevier 26(3): 471–480.

Liu M, Frangopol DM, and Kim S (2009). "Bridge system performance assessment from structural health monitoring: A case study." J Struct Eng, ASCE 135(6):733–742

Madsen HO, Torhaug R, Cramer EH (1991) Probability-based cost benefit analysis of fatigue design, inspection and maintenance. Proceedings of the Marine Structural Inspection, Maintenance and Monitoring Symposium, SSC/SNAME, Arlington, VA., II.E.1–12

Martinez-Luengo M, Kolios A, Wang L (2016) Structural health monitoring of offshore wind turbines: a review through the statistical pattern recognition paradigm. Renew Sust Energ Rev Elsevier 64:91–105

MathWorks (2016) Optimization toolbox™ User's guide. MathWorks, Natick

Meo M, Zumpano G (2005) On the optimal sensor placement techniques for a bridge structure. Eng Struct Elsevier 27(10):1488–1497

Mohanty JR, Verma BB, Ray PK (2009) Prediction of fatigue crack growth and residual life using an exponential model: part I (constant amplitude loading). Int J Fatigue Elsevier 31(3):418–424

Myers JL, Well AD, Lorch RF Jr (2003) Research design and statistical analysis. Routledge, New York

NCHRP. (2003) Bridge life-cycle cost analysis. NCHRP-report 483, Transportation Research Board, Washington D.C.

NCHRP (2006) Manual on service life of corrosion-damaged reinforced concrete bridge superstructure elements. NCHRP-report 558, Transportation Research Board, Washington D.C.

NCHRP (2012) Estimating life expectancies of highway assets – Volume 1: Guidebook. NCHRP-report 713, Transportation Research Board, Washington D.C.

Orcesi AD, Frangopol DM (2011) Optimization of bridge maintenance strategies based on structural health monitoring information. Struct Saf Elsevier 33(1):26–41

Paris P, Erdogan F (1963) A critical analysis of crack propagation laws. J Basic Eng ASME 85(4):528–533

Pohekar SD, Ramachandran M (2004) Application of multi-criteria decision making to sustainable energy planning—a review. Renew Sust Energ Rev Elsevier 8(4):365–381

Sabatino S, Frangopol DM (2017) Decision making framework for optimal SHM planning of ship structures considering availability and utility. Ocean Eng Elsevier 135:194–206

Sánchez-Silva M, Frangopol DM, Padgett J, Soliman M (2016) Maintenance and operation of infrastructure systems: review. J Struct Eng ASCE 142(9):F4016004

Saxena DK, Duro JA, Tiwari A, Deb K, Qingfu Z (2013) Objective reduction in many-objective optimization: linear and nonlinear algorithms. Evol Comput IEEE 17(1):77–99

Soliman M, Barone G, Frangopol DM (2014) Fatigue reliability and service life prediction of aluminum naval ship details based on monitoring data. Struct Health Monit SAGE 14(1):3–19

Soliman M, Frangopol DM, Mondoro A (2016) A probabilistic approach for optimizing inspection, monitoring, and maintenance actions against fatigue of critical ship details. Struct Saf Elsevier 60:91–101

Thoft-Christensen P, Sørensen JD (1987) Optimal strategy for inspection and repair of structural systems. Civ Eng Environ Syst Taylor & Francis 4(2):94–100

Wang Y-M, Luo Y (2010) Integration of correlations with standard deviations for determining attribute weights in multiple attribute decision making. Math Comput Model Elsevier 51(1–2):1–12

Worden K, Burrows AP (2001) Optimal sensor placement for fault detection. Eng Struct Elsevier 23(8):885–901

Yoon KP, Hwang C-L (1995) Multiple attribute decision making: an introduction. SAGE Publication Inc., London

Zavadskas EK, Turskis Z, Kildienė S (2014) State of art surveys of overviews on MCDM/MADM methods. Technol Econ Dev Econ Taylor & Francis 20(1):165–179